

# Creating vortex retarders using photoaligned liquid crystal polymers

Scott C. McEldowney,<sup>1,\*</sup> David M. Shemo,<sup>1</sup> Russell A. Chipman,<sup>2</sup> and Paula K. Smith<sup>2</sup>

<sup>1</sup>JDSU, 2789 Northpoint Parkway, Santa Rosa, California 95407, USA

<sup>2</sup>University of Arizona, College of Optical Sciences, Tucson, Arizona 85721, USA

\*Corresponding author: scott.mceldowney@jdsu.com

Received October 22, 2007; revised December 5, 2007; accepted December 5, 2007;  
posted December 10, 2007 (Doc. ID 88916); published January 9, 2008

We present developments using photoaligned liquid crystal polymers for creating vortex retarders, half-wave retarders with a continuously variable fast axis. Polarization properties of components designed to create different polarization vortex modes are presented. We assess the viability of these components by using the theoretical and experimental point spread functions in Mueller matrix format, or a point spread matrix (PSM). The measured PSM of these components in an optical system is very close to the theoretically predicted values, thus showing that these components should provide excellent performance in applications utilizing polarized optical vortices. © 2008 Optical Society of America

OCIS codes: 230.0230, 230.5440, 230.3720.

Optical fields that are linearly polarized and axially symmetric are becoming very important in the design of advanced optical systems. In the case of radially or azimuthally polarized beams, they have been shown to improve performance in confocal microscopy [1] and lithography systems [2]. More general polarization vortices of single or higher orders can be used to create nondiffracting or Bessel fields [3]. One emerging application of Bessel beams is in enlarging the particle trapping region of optical tweezers [4].

Traditionally, these fields are made by using coherent interference of TE and TM modes [5]. Recently, components that utilize a constant retardance but variable fast axis have demonstrated the potential of monolithic components to create such vortex fields [2,6,7]. We define a vortex retarder as a monolithic component that has a constant retardance but a fast axis that rotates about a point. A plurality of crystals can be assembled to make a vortex retarder [7]. However, the fast axis cannot be made continuous, therefore causing diffraction at the boundaries of the different crystals forcing the use of additional components to create a pure polarization vortex. The assembly process is also complex, making the components expensive. Vortex retarders made from nanostructures [3] have the potential to create stable retarders with a continuous fast axis and, in principle, can be made over broad wavelength ranges. However, the feature sizes required for making visible vortex retarders is beyond state-of-the-art of feature generation and thus has been demonstrated only at infrared wavelengths. Vortex retarders made by using twisted nematic liquid crystal [6] are limited in that, thus far, multiple components are required if polarization vortices beyond order 2 are required.

Liquid crystal polymers (LCPs) are materials that combine the birefringent properties of liquid crystals with the mechanical properties of polymers. The orientation of a LCP is achieved through the use of an alignment layer [8]. Photoalignment is a recent advancement that enables noncontact alignment, which produces high-quality alignment with low defects as

compared with rubbing alignment techniques [8]. Photoalignment also allows a high degree of customization in producing birefringent components. Once the alignment orientation has been established in the alignment layer, the LCP precursor is applied and cross-linked to make its orientation permanent.

In this Letter, we describe the development of a vortex retarder using a photo-aligned LCP. We demonstrate vortex retarders, half-wave retarders with a continuously varying fast axis, creating  $m=1, 2, 3$  vortex modes at 550 nm. We analyzed these elements both theoretically and experimentally by measuring the space variant Mueller matrix of each component. The viability of these components is assessed by determining the Mueller matrix of the point spread function (PSF) or point spread matrix (PSM); the combination of these allows us to fully understand the optical vortex created by the component and its impact in an optical system. The PSM is a Mueller matrix for which each element of the matrix is a PSF.

The Jones matrix for a vortex retarder is

$$\mathcal{J}[\varphi] = \begin{pmatrix} \cos(m\varphi) & \sin(m\varphi) \\ \sin(m\varphi) & -\cos(m\varphi) \end{pmatrix}, \quad (1)$$

where  $\phi$  is the azimuthal angle of the component and  $m$  is the output mode of the field. The fast axis orientation of the vortex retarder is described as a linear relationship,

$$\theta = \alpha\phi + \delta, \quad (2)$$

where  $\theta$  is the fast axis orientation at a given azimuthal angle ( $\phi$ ) on the component,  $\alpha$  is the rate of change in  $\theta$  with respect to  $\phi$ ,  $\delta$  is the fast axis orientation at  $\phi=0$ , and  $m$  is related to  $\alpha$  by  $m=2\alpha$ . To make the  $m=1, 2, 3$  vortex retarders, we used a value of  $\alpha$  of 1/2, 1, and 3/2, respectively.

The samples were fabricated on 2 in. (1 in. = 2.54 cm) squares of Corning 1737F glass, having a broadband visible antireflection coating on the back surface. The process targeted a half-wave retardance

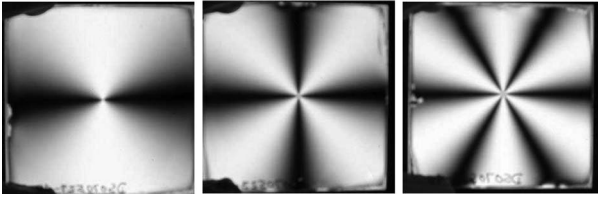


Fig. 1. Vortex retarders of  $m=1, 2, 3$  analyzed through a linear polarizer.

for wavelengths in the range of 540–550 nm. A photoalignment layer (ROP108 from Rolic) was spin coated onto the substrate and baked, and then the alignment was set through exposure to linear polarized UV light. We exposed the alignment layer through a narrow wedge-shaped aperture located between the substrate and the polarizer. Both the polarizer and the substrate were continuously rotated during the exposure process to create a continuous variation in photoalignment orientation with respect to azimuthal locations on the substrate. The desired  $\alpha$  slopes in Eq. (1) were determined by the relative rotation speeds. The LCP precursor (ROF5104 from Rolic) was then spin coated and subsequently polymerized by using a UV curing processes. The orientation of the LCP is set by the orientation of the alignment layer. The retardance value depends on the thickness of LCP.

Examining the three samples in white light between crossed polarizers produces the results shown

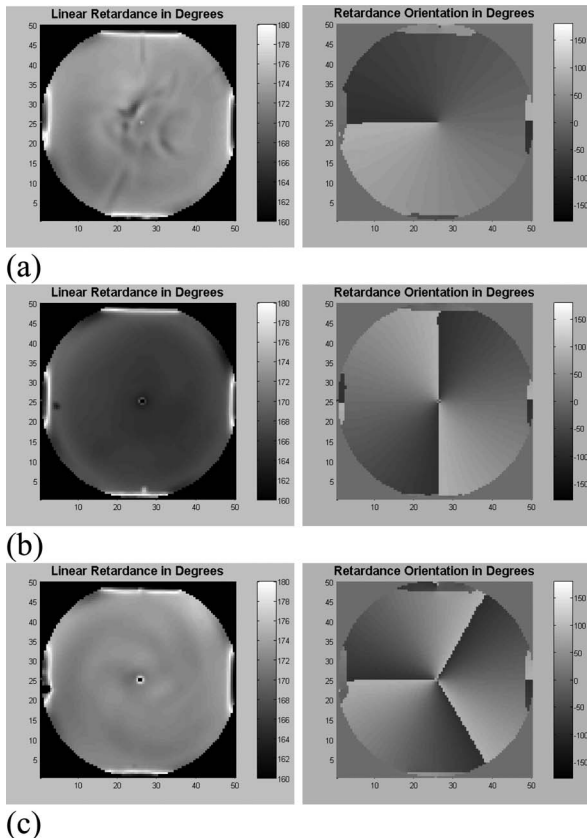


Fig. 2. Retardance (left) and fast axis (right) for (a) the  $m=1$  component, (b) the  $m=2$  component, and (c) the  $m=3$  component. In all cases the retardance is measured in degrees at  $\lambda=570$ , and the fast axis is in degrees.

in Fig. 1. Figure 1 clearly shows the modulation of intensity expected. The number of modulations is as expected for each component, with  $m=1$  having 2 modulations,  $m=2$  having 4, and  $m=3$  having 6.

The samples were mapped using a Mueller matrix polarimeter from Axometrics at a 1 mm pitch in an  $x-y$  map. The retardance and fast axis maps are shown in Fig. 2 for the  $m=1, 2, 3$  vortex retarders. The irregularities seen at the top, bottom, left, and right of the retardance and fast axis maps are merely artifacts of the retardance order changing from order 0 to order 1 where the LCP becomes thicker near the substrate edge. (The retardance map analysis here assumes order 0 for all locations.) Although a few minor coating artifacts are present in the retardance maps, the samples show excellent retardance uniformity (nonuniformity less than 2.5%); the fast axis is continuous at the scale that the parts were mapped.

To determine the effectiveness of these vortex retarders, we measured the PSM and compared this with calculated values. To calculate the PSM in the case of a paraxial system, we followed the technique of McGuire and Chipman [9]. The amplitude response matrix ( $h$ ) for a polarizing system containing a single or group of lenses is determined by taking the Fourier transform of the Jones matrix of the vortex retarder and multiplying by a quadratic phase factor between the object and the image.

To convert the amplitude response matrix to the PSM, we use the relationship

$$P = h \otimes h^*, \quad (3)$$

where  $\otimes$  indicates the direct product [9]. To convert to the Stokes basis, we use the transformation

$$P_s = SPS^{-1} \quad (4)$$

where  $S$  is a transformation matrix [9].

To measure the PSM, we used a Mueller matrix imaging polarimeter [10] and set the CCD camera image plane conjugate to fiber optic illumination. The measurements were made at 550 nm where the vortex retarders were approximately a half-wave. The

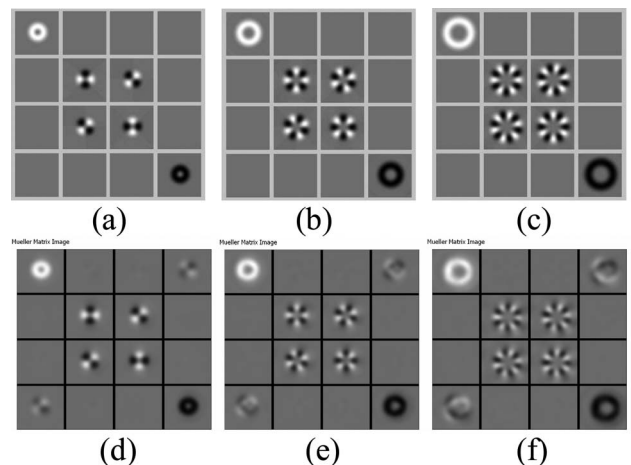


Fig. 3. (a)–(c) Calculated PSM and (d)–(f) Measured PSM for the  $m=1, 2, 3$  vortex retarders.

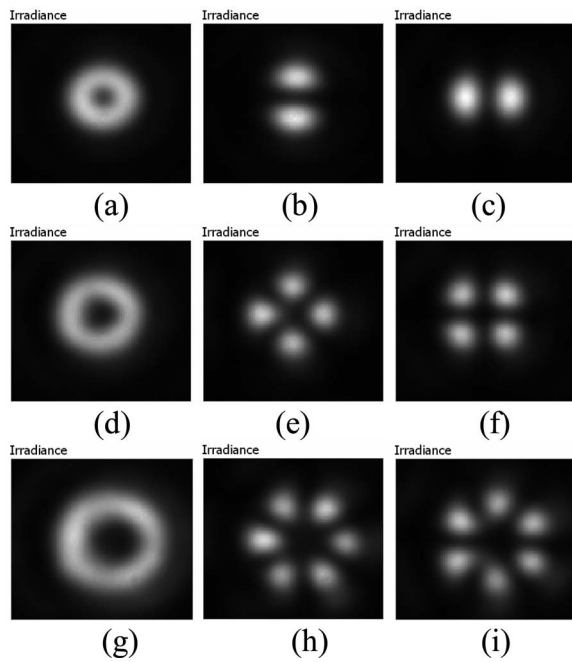


Fig. 4. (a) Irradiance of the (a)  $m=1$ , (d)  $m=2$ , and (g)  $m=3$  vortex retarder measured intensity; (b), (e), (h), corresponding HLP input and HLP analyzer; (c), (f), (i) with HLP input and VLP analyzer.

vortex retarder was uniformly illuminated over a diameter of approximately 2.5 mm.

Figure 3 shows the calculated and the measured PSM for the three vortex retarders. The results show very good qualitative agreement between the measured PSM and the calculated PSM. The only exception is the higher than predicted value in the  $m03$  and  $m30$  elements of the PSM. Further analysis suggests that this is partially due to the center area ( $< \sim 100 \mu\text{m}$ ) of the vortex retarder where the orientation becomes disordered. The impact of these elements is to increase the circular polarization and circular polarizance of the component.

With the PSM measured, it was trivial to determine the field generated at the image plane for a va-

riety of input polarization states and output analyzers. As an example, Fig. 4 shows the intensity at the image plane for each of the vortex retarders for three conditions based on the measured PSM; arbitrary input with arbitrary output, horizontal linear polarized input with horizontal linear polarized output, and horizontal linear polarized input with vertical polarized output.

The PSFs shown in Figs. 4(a), 4(d), and 4(g) show the expected doughnut-shaped profile. The PSF function measured when an analyzer is used shows a propeller-shaped profile with the rotation of the propeller depending on the order of the vortex retarder.

In conclusion, we have demonstrated that we can make vortex retarders for visible wavelengths by using photoaligned LCP materials. The fast axis can be made continuous such that vortex retarders of single or multiple modes can be manufactured. The measured PSM of these components in an optical system is very close to the theoretically predicted values, thus showing that these components should provide excellent performance in applications utilizing polarized optical vortices.

## References

1. R. Dorn, S. Quabis, and G. Leuchs, *Phys. Rev. Lett.* **91**, 233901 (2003).
2. X. Grosjean, D. Courjon, and C. Bainier, *Opt. Lett.* **32**, 976 (2007).
3. A. Niv, G. Biener, V. Kleiner, and E. Hasmin, *Opt. Lett.* **29**, 238 (2004).
4. D. McGloin and K. Dholakia, *OE Mag.* January, 2003, pp. 42–45.
5. S. C. Tidwell, D. H. Ford, and W. D. Kimura, *Appl. Opt.* **29**, 2234 (1990).
6. M. Stalder and M. Schadt, *Opt. Lett.* **21**, 1948 (1996).
7. G. Machavariani, Y. Lumer, I. Moshe, A. Meir, and S. Jackel, *Opt. Lett.* **32**, 1468 (2007).
8. M. Schadt, H. Seiberle, A. Schuster, and S. M. Kelly, *Jpn. J. Appl. Phys., Part 1* **34**, L764 (1995).
9. J. P. McGuire, Jr., and R. A. Chipman, *J. Opt. Soc. Am. A* **7**, 1614 (1990).
10. J. L. Pezzaniti and R. A. Chipman, *Opt. Eng.* **34**, 155 (1995).